Chemistry & Biology *13*, 569–574, June 2006 DOI 10.1016/j.chembiol.2006.05.010

Asteropine A, a Sialidase-Inhibiting Conotoxin-like Peptide from the Marine Sponge *Asteropus simplex*

Brief Communication

Kentaro Takada,[1] Toshiyuki Hamada,[2,3] Hiroshi Hirota,[2,3] Yoichi Nakao,[1] Shigeki Matsunaga,[1] Rob W.M. van Soest,[4] and Nobuhiro Fusetani[1,*]

[1] Laboratory of Aquatic Natural Products Chemistry
Graduate School of Agricultural and Life Sciences
The University of Tokyo
Japan

[2] Genomic Sciences Center (GSC)
RIKEN (The Institute of Physical and Chemical Research)
Japan

[3] Division of Protein Folds Research
Graduate School of Integrated Science
Yokohama City University
Japan

[4] Institute for Systematics and Ecology
University of Amsterdam
The Netherlands

Summary

Marine sponges contain structurally intriguing and biologically active peptides of nonribosomal peptide synthase origin, often containing amino acids with novel structures. Here we report the discovery of asteropine A (APA), a cystine knot to be isolated from marine sponges. The solution structure of APA as determined by NMR belongs to the four-loop class of cystine knots similar to those of some conotoxins and spider toxins. However, the highly negatively charged surface of APA is uncommon among other cystine knots. APA competitively inhibits bacterial sialidases, but not a viral sialidase. APA was inactive against all other enzymes tested and did not have any apparent antitumor activity. Our data suggest that APA and other knotting peptides may be important leads for antibacterial and even antiviral drug development.

Introduction

Sialic acids are placed at the terminal position of complex carbohydrate chains on the cell surface of higher animals. They are believed to play structural roles in connection with their unique acidic character and bulkiness by physically protecting the surface of cells from extracellular damaging agents. Sialic acids also function structurally to mask the penultimate galactose residue, which is often targeted in physiological or pathological recognition events. Sialidases, which are present in higher animals, are enzymes that hydrolyze the terminal sialic acid residue of complex carbohydrate chains. The enzymes are widely conserved in microorganisms, such as viruses, bacteria, fungi, and protozoa, which are associated with higher animals. Because of the limited occurrence of sialidases and sequence homology of these enzymes across different phyla, microbial sialidases are considered to be acquired through horizontal gene transfer between the host and microbe [1]. Although not much is known about the function of bacterial sialidases, their pathological roles are implicated in *Vibrio cholerae*, *Salmonella typhimurium*, and *Clostridium* spp [2].

The development of viral sialidase inhibitors provides an example of an attractive strategy for designing ligands on the basis of the target protein structure [3]. However, though potent inhibitors of the influenza enzyme have been developed, they are not potent against bacterial enzymes. Structural differences between the bacterial sialidases and their viral homologs have prevented the design of effective bacterial inhibitors based on homology modeling. To date, several inhibitors that are selective for bacterial sialidases are known. Siastatins A and B from *Streptomyces verticillus* var. *quintum* are competitive inhibitors of the *C. perfringens* sialidase, but are inactive against the *V. cholerae* sialidase [4]. Taurolipids A and B from *Tetrahymena* spp. are noncompetitive inhibitors of the *C. perfringens* sialidase with no inhibitory activity against the corresponding *Arthrobacter ursafacience* and *Streptococcus* enzymes [5].

In the course of screening bioactive metabolites from marine invertebrates for inhibitory activity against sialidase, we previously have reported two new classes of metabolites [6, 7]. An additional activity was observed in the extract of the sponge *Asteropus simplex*, collected off Shikine-jima Island, 200 km south of Tokyo. Bioassay-guided fractionation of the extract afforded asteropine A (APA), as the principal active constituent. This paper describes the isolation, structure elucidation, solution structure, and enzyme inhibitory activity of APA.

Results and Discussion

Sequence Analysis of Asteropine A

Asteropine A (APA) was isolated from an extract of the marine sponge *Asteropus simplex* as the major sialidase inhibitory constituent. The matrix-assisted laser desorption ionization time-of-flight mass spectrometry (MALDI-TOFMS) of APA exhibited an ion peak at *m/z* 3817.5 corresponding to the $(M+H)^+$ ion. The NMR spectra in CD_3OH exhibited numerous amide and aliphatic signals, which indicated peptidic nature of the active compound. APA was reduced with tri-*n*-butylphosphine (TBP) and alkylated with 4-vinylpyridine (4-VP) because the presence of Cys was revealed by the amino acid analysis. The alkylated product (6PE-APA) gave an ion peak at *m/z* 4456.7 Da, consistent with the introduction of six pyridylethyl groups after reduction of three disulfide bonds. Edman degradation analysis of 6PE-APA gave the sequence of 30 residues from the N terminus: YCGLF GDLCT LDGTL ACCIA LELEC IPLND. To determine the sequence of the remaining portion, 6PE-APA was digested with V8 protease and the products were separated by RP-HPLC to afford a C-terminal 1516 Da dodecapeptide fragment. The combination of post

*Correspondence: anobu@mail.ecc.u-tokyo.ac.jp

source decay analysis (PSD) by the MALDI-TOFMS and Edman degradation analysis revealed that the sequence of this fragment was CIPLNDFVGICL. The complete amino acid sequence was confirmed by an independent NMR analysis of 6PE-APA. The ^{1}H NMR spectrum of 6PE-APA in DMSO-d_6 shows a typical pattern of a peptide in a random coil conformation as characterized by small coupling constants between NH and Hα and less dispersed and shielded Hα signals [8, 9]. Nuclear overhauser effects (NOEs) in 6PE-APA were observed mainly between neighboring residues throughout the sequence without severe overlaps, allowing an unambiguous sequential assignment to be established. The NMR spectra also indicated the absence of any posttranslational modifications in APA. The stereochemistry of all component amino acids was determined to be L on the basis of gas chromatography (GC) analysis of the acid hydrolyzate using a chiral stationary phase. This sequence has no homology to any protein, peptide, or translated nucleotide sequence in the BLAST database.

Secondary Structure

Although virtually insoluble in water, APA was highly soluble in CD_3OH and gave sharp ^{1}H NMR signals. In the ^{1}H NMR spectrum of APA measured in CD_3OH, both the NH and Hα signals were dispersed, indicating that the peptide was well structured. Sequence specific chemical shift assignments were made for all ^{1}H NMR signals according to standard methods [10, 11]. NOESY data, $^{3}J_{NH\text{-}H\alpha}$ values, and chemical shift indices (CSI) [12, 13] of Hα were used to define secondary structures (Figure 1A). These data indicate the presence of β strands comprising residues (8–10, 15–17, 23–26, and 31–34), turns, and a small stretch of helix between the second and third strands. The first, third, and fourth strands form a triple stranded antiparallel β sheet as identified by the relevant long-range connectivities (Figure 1B).

Because all available proteases were unable to digest the intact peptide, connectivities of the three disulfide bonds were analyzed by the combination of NOESY data and chemical method. Statistical analyses of proton-proton distance in crystal structures were reported [14], showing only NOE correlations between Hβ-Hβ and Hα-Hβ indicated a positive prediction for the characterization of disulfide bonding pattern. ($d_{\beta\beta}$ < 4.0 Å, 95.7% of cysteines form a pair, $d_{\beta\beta}$ < 5.0 Å, 88.8%). In the case of APA, there were three Hβ-Hβ'NOE interactions observed between Cys17/Cys35 (2 NOEs) and between Cys9/Cys25, which strongly suggested that cysteine pairs were C17/C35 and C9/C25. A range of other NOEs between cysteines (C17 NH/C9 H β1, C17 NH/C25 H β1, C18 NH/C2 H β1, C35 αH/C25 H α) was also observed. These NOEs were neither definitive for nor inconsistent with the proposed connectivity according to the literature. By default the third disulfide was between Cys2 and Cys18. This assignment was supported by the Gray's method [15] of a partial reduction followed by alkylation and then a secondary reduction followed by a different mode of alkylation.

Three-Dimensional Structure

The solution structure of APA was established by 2D NMR analysis and simulated annealing calculations within the program CNS [16]. The 20 structures with

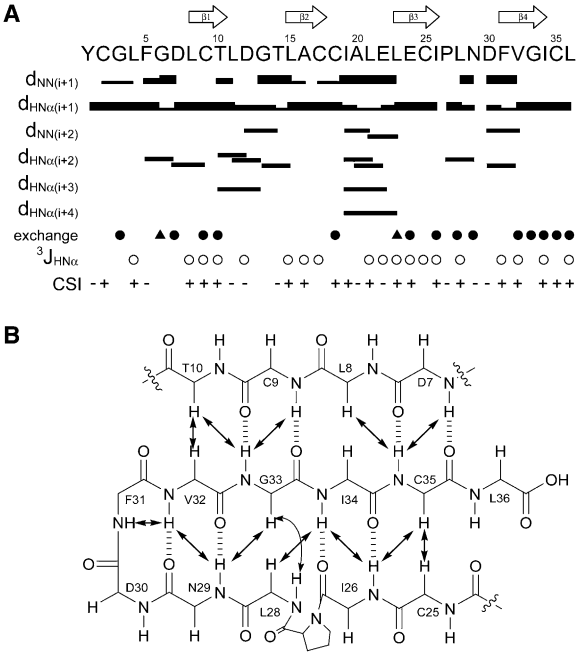

Figure 1. Identification of the Secondary Structure Elements of APA

(A) The sequential and medium range NOE correlations (i-j < 5) were represented by solid lines connecting the two residues. NOE intensities are grouped into 3 classes and represented by the heights of bars. Filled circles indicate the position of amide protons hardly exchanged after 72 hr and filled triangles indicate the positions of amide protons partially exchanged after 72 hr. Open circles indicate the position where $^{3}J_{NH\text{-}H\alpha}$ values are larger than 8 Hz. The chemical shift index [12, 13] is also indicated with (+) and (−) signs. The arrows at the top of the figure indicate the position of β strands as indicated by NMR analysis. For the residues in the strands, most $^{3}J_{NH\text{-}H\alpha}$ values were larger than 8 Hz and NH-NH$_{i+1}$ connectivities were weak.

(B) Triple-stranded antiparallel β sheet region in APA. NOE correlations (solid arrows) and hydrogen bonds (dashed line) are indicated.

the lowest energies and no residual restraint violations were chosen to represent the solution structure of APA (Figure 2B). The rmsd value of the backbone atoms and heavy atoms for residues 2–35 were 0.27 and 0.78 Å, respectively. The summary of geometric statistics shown in the Experimental Procedures indicates that the structures are consistent with the experimental restraints. The molecule has four loops each bound by half-cystine residues and the central part of each loop forms a β turn. The hydrophobic core is composed of a cystine knot motif, in which Cys17-Cys35 disulfide bond passes through a ring formed by Cys2-Cys18 and Cys9-Cys25. As is often the case with peptides containing this motif, there is a triple-stranded antiparallel β sheet (topology: +2x, −1, Figure 2C). These secondary structural features are also the similar as those observed in the solution structure of many of spider toxins or conotoxins (Figure 2D).

Cystine knots are widely distributed in organisms ranging from fungi, plants, and invertebrates, to vertebrates [17]. From a functional point of view, these peptides are often associated with chemical defense of the producing organisms by exhibiting antimicrobial,

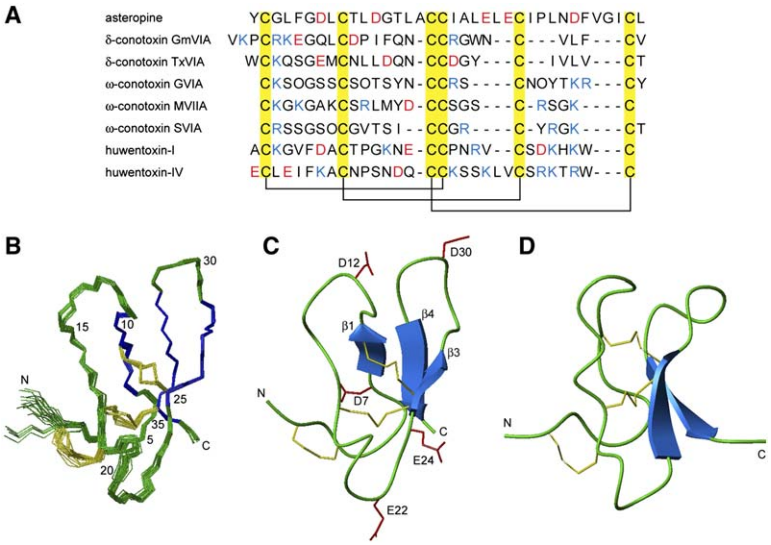

Figure 2. Sequence and Solution Structure of APA

(A) Sequence alignment of APA with δ-conotoxin GmVIA [24], δ-conotoxin TxVIA [25], ω-conotoxin GVIA [26], ω-conotoxin MVIIA [27], ω-conotoxin SVIA [28], Huwentoxin-I [29], and Huwentoxin IV [30]. Blue and red characters indicate basic and acidic amino acids, respectively. The cysteine residues are highlighted by yellow rectangles, and the disulfide bonds are connected by solid lines. O indicates hydroxyproline.

(B) The backbone atoms of all residues for the family of 20 structures of APA best fitted to N, Cα, and C′ atoms. A total of 300 distance constraints (97 intraresidual, 110 sequential, 37 medium-range, and 56 long-range) and 19 backbone dihedral angle constraints derived from NH-Hα coupling constants were used for the calculation. At a late stage of calculations, hydrogen bonds in the β sheet as confirmed from preliminary calculations were added. The rmsd value of the backbone atoms and all heavy atoms for residues 2–35 were 0.27 and 0.78 Å, respectively. The three disulfide bonds and a triple-stranded antiparallel β sheet are colored yellow and blue, respectively. Every fifth residue is labeled with residue number.

(C) Ribbon representation of the model of the solution structure of APA with the lowest energy, showing the regular secondary structures and global fold of the peptide. The side chains of six half cystine residues are shown and colored yellow. Acidic amino acids were colored red. This figure was drawn with the program MOLMOL [31].

(D) Huwentoxin IV [30] (Protein Data Bank code: 1MB6) was drawn by the same manner as that of APA.

enzyme inhibitory, or ion-channel binding activity. Conotoxins, especially, were discovered as active components of *Conus* venom, each of which has specific activity for certain cation channels [18]. In spite of their relatively small size, this class of peptides is highly structured due to the presence of the disulfide bond network. The structural folds in these peptides are largely governed by the distribution of cysteine residues in the chain and the connectivities of the disulfide bonds. Therefore, the conceptual framework of cystine knot has been suggested to be a technological platform for drug discoveries.

Interestingly, APA is a highly acidic peptide with six acidic groups including the C terminus and one basic group N terminus, whereas other cystine knots, particularly toxic peptides, are generally highly basic reflecting their function of blocking cationic channels (Figure 2A). Charged and hydrophobic residues are more or less evenly distributed on the surface of the molecule. It is likely that one or more acidic functional groups in APA are necessary to inhibit sialidases, as is the case of other sialidase inhibitors. Although numerous cystine-rich peptides with potent biological activities have been isolated, this is the first example of a peptide predominantly acidic in nature.

Marine sponges are widely recognized to be an important source of biologically active small molecules. In the characterization of peptides and proteins from marine sponges, it has been observed that many peptides are of nonribosomal origin. Despite the fact that some of these proteins have been identified as biologically active with activities ranging from cytotoxicity, calcium channel blocking activity, and inhibition of HIV infection [19], it is not known whether these peptides are coded in the genome. In the case of conotoxins isolated from the venom of marine snails, it has been determined that they are initially biosynthesized as 70–120 amino acid peptides, followed by both posttranslational modification and proteolytic cleavage to produce a variety of small peptides. The structural similarities between APA and conotoxins imply that APA may have the same biosynthetic pathway. In addition, we assume that APA has a biological function in the organism, because it is contained in a large amount (2.1×10^{-3} % based on wet tissue) in the sponge and of ribosomal origin.

Inhibitory Activities against Sialidases and Other Enzymes

APA is a potent competitive inhibitor of bacterial sialidases. The competitive mode of inhibition and the K_i value of 36.7 nM for *C. perfringens* were indicated by a Lineweaver-Burk and a Dixon plot (Figure 3). APA competitively inhibits sialidases from *V. cholerae* and S. *typhimurium* with K_i values of 340 nM and 350 nM, respectively. However, APA was inactive not only against sialidase from influenza A virus (H3N2) at 30 μM, but also other glycosidases, e.g., α-glucosidase, β-glucosidase, and β-galactosidase and proteases, e.g., trypsin, chymotrypsin, papain, thrombin, and leucineaminopeptidase at a concentration of 30 μM. Similarly, APA was not cytotoxic against P388 and HeLa cells at 5 μM (Table 1). Thus, the action of APA is highly selective toward bacterial sialidases.

Significance

Bioassay-guided fractionation of the extract of the marine sponge *Asteropus simplex* afforded a novel 36 residue peptide, aseteropine A, as a bacterial sialidase inhibitor. The solution structure study of asteropine A implied that it is the first cystine knot isolated from marine invertebrates other than the cone snail. The

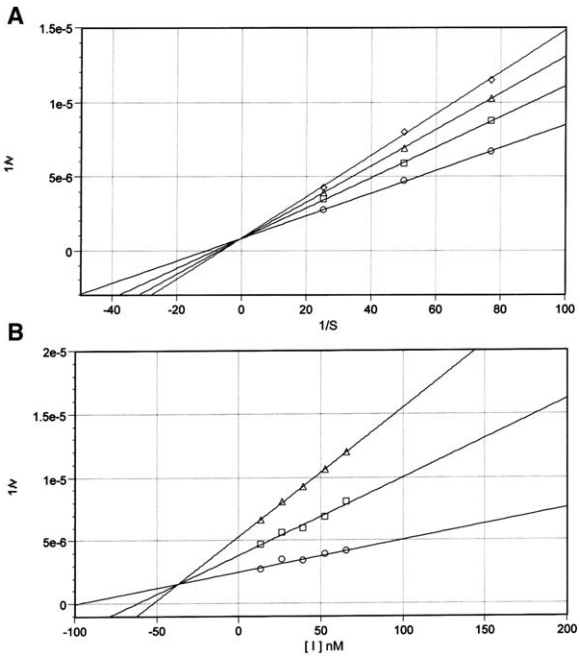

Figure 3. Lineweaver-Burk and Dixon Plot Analysis of APA against *C. perfringens* Sialidase

The inhibitory activity of APA was determined by observing the release of 4-methyl umbelliferone as described in the Experimental Procedures.

(A) Lineweaver-Burk plot, four different concentrations (C, 13 nM; Δ, 26 nM; G, 52 nM; I 65nM) of APA yielded straight lines crossing each other on the y axis, indicating the competitive mode of inhibition.

(B) Dixon plot, three different concentrations (C, 0.04 mM; G, 0.02 mM; Δ, 0.013mM) of substrate were carried out. The point crossing by each line is 36.7 nM.

present study also proved that a peptidic molecule has ability to be a potent sialidase inhibitor. Recently, threats of viral diseases such as, avian flu [20], HIV and Ebola, have become increasingly serious public health concerns. The need to develop effective measures against these viral diseases carries some urgency. We believe that an effective strategy in antiviral drug development is further exploration of chemistries associated with the cystine knot framework highly inhibiting viral infections. Further investigation of APA is an important first step in this process.

Table 1. Biological Activities of APA

	K_i value
Sialidase	
C. perfringens	36.7 nM (competitive)
V. cholerae	340 nM (competitive)
S. typhimurium	350 nM (competitive)
Influenza A/Memphis/71(H3N2)	inactive

APA showed no inhibiton for any other glycosidases (α-glucosidase, α-glucosidase, β-galactosidase) and proteases (trypsin, chymotorypsin, papain, thrombin, leucin amino peptidase) at the concentration of 30 μM. APA also showed no cytotoxicity for HeLa and P388 cell lines at the concentration of 5 μM.

Experimental Procedures

General Procedure

Optical rotation was measured on a JASCO DIP-1000 digital polarimeter. MALDI-TOFMS were measured using PerSeptive Biosystems Voyager-DE STR operated in the positive ion reflector and linear modes and the data were analyzed using PerSeptive Biosystems Data Explorer ver.3.2. Either α-cyano-4-hydroxy cinnamic acid or sinapinic acid was used as a matrix. IR spectrum was recorded on a JASCO FT/IR-5300 spectrometer. Fluorescence for inhibition assay was measured with a Molecular Device Spectra MAX GEMINI apparatus.

Animal Materials

The sponge was collected by hand using SCUBA at depths of 10–15 m off Shikine-jima Island of the Izu Archipelago (34°20′N, 139°13′E) and kept frozen at –20°C until extraction. The sponge was identified as *Asteropus simplex* (order Astrophorida, class Geodiidae). A voucher specimen was deposited at the Zoological Museum of University of Amsterdam (ZMA 16718).

Isolation of APA

The sponge *Asteropus simplex* (1.1 kg) was homogenized in MeOH and sequentially extracted with MeOH (2 liter x 2), EtOH (2 liter x 1), and acetone (2 liter x 1). The combined extracts were concentrated and partitioned between H_2O and Et_2O. The H_2O layer was further partitioned between H_2O and *n*-BuOH and the *n*-BuOH fraction was separated by ODS flash chromatography with mixtures of H_2O and MeOH, followed by gel filtration on a Sephadex LH-20 column (5 × 100 cm) with CH_2Cl_2/MeOH (1:1). The active fraction was purified by reversed-phase HPLC (Cosmosil 5C_{18}-ARII, ϕ20 × 250 mm) with a linear gradient elution from MeCN-H_2O-TFA (30:70:0.1 to 60:40:0.1). The final purification of an active fraction was performed by reversed-phase HPLC (Develosil C_{30}-UG5, ϕ20 × 250 mm) with MeCN-H_2O-TFA (48:52:0.1) to afford APA (23.5 mg, 2.1 × 10^{-3} % yield based on wet weight). The peptide sequence data was registered in the UniProt Knowledgebase under the accession number P84702.

APA: white powder; $[\alpha]^{20}_D$ = +13° (*c* 0.10, MeOH); IR (film) 3287, 2923, 1660, 1537, 1455, 1395, 1259, 700 cm^{-1}, MALDI-TOFMS 3817.5 $(M+H)^+$.

NMR Spectroscopy

NMR samples were prepared by dissolving 2mM APA in 180 μl of CD_3OH and measured either on a Bruker Avance 800 MHz or on a JEOL Alpha 600 NMR spectrometer. Water suppression in the NOESY and HOHAHA spectra was achieved using a modification of a WATERGATE sequence [21]. ^1H and ^{13}C NMR chemical shifts were referenced to the solvent peaks: δ_H 3.30 and δ_C 49.0 for CD_3OH, and δ_H 2.40 and δ_C 40.0 for DMSO-*d*6. The intact peptide was analyzed by DQF-COSY, HOHAHA, HMQC, HMBC, and NOESY spectra.

Complete Reduction Followed by Alkylation with 4-Vinylpyridine

A 5 mg portion of APA was dissolved in 1 ml of 0.5 M Tris-acetate buffer (pH 8.5) containing 7 M guanidine hydrochloride and 10 mM EDTA. To the solution were added 4-vinylpyridine (10 μl) and tri-*n*-butylphosphine (20 μl), and the mixture was kept under an atmosphere of N_2 in the dark at rt for 24 hr. The reaction mixture was purified by reversed-phase HPLC (Cosmosil 5C_{18}-ARII, ϕ20 × 250 mm) with a linear gradient elution from MeCN-H_2O-TFA (30:70:0.1 to 50:50:0.1) to afford 2.5 mg of the hexapyridylethyl derivative. MALDI-TOFMS data [*m/z* 4456.7 $(M+H)^+$] was in agreement with introductions of six 4-pyridylethyl groups.

Gas Chromatography

A 0.2 mg portion of APA was dissolved in 200 μl of 6 N HCl and hydrolyzed at 110°C for 12 hr. The solution was dried in a stream of N_2, and redissolved in 200 μl of 10% HCl-MeOH, and kept at 110°C for 2 hr. A half portion of the product was dissolved in CH_2Cl_2/trifluoroacetic anhydride (1:1, 100 μl) and kept at 100°C for 10 min. The reaction mixture was dried in a stream of N_2, dissolved in CH_2Cl_2, and subjected to GC analysis. The remaining half portion of the

reaction mixture was dissolved in MeCN-H_2O-TFA (60:40:0.1) and treated with TBP (20 μl) for 1 hr at 60ºC followed by partitioning between H_2O and *n*-BuOH, so that cystine was reduced to cysteine. The organic phase was trifluoroacetylated as described above and dissolved in CH_2Cl_2. An aliquot of each solution was subjected to GC analysis on a Chirasil-L-Val capillary column (0.25 mm × 25 m): detection, FID; initial temperature 60ºC for 6 min., final temperature 200ºC for 1 min., temperature raised at 4ºC $min.^{-1}$; carrier gas, He. Retention times for standard amino acids (min): D-Ala (9.6), L-Ala (11.3), D-Val (13.0), L-Val (14.0), D-Thr (14.6), D-*allo*-Thr (15.7), L-Thr (16.0), L-*allo*-Thr (17.0), D-Pro (17.0), L-Pro (17.3), D-Ile (16.5), D- *allo*-Ile (19.6), L-Ile (17.5), L-*allo*-Ile (21.0), D-Leu (19.0), L-Leu (20.7), D-Asp (22.4), L-Asp (22.9), D-Cys (25.5), L-Cys (26.2), D-Phe (28.2), L-Phe (29.1), D-Glu (29.6), L-Glu (30.5), D-Tyr (36.3), L-Tyr (37.0). Retention times for the acid hydrolyzate of APA (min): 11.1, 13.7, 15.8, 17.2, 17.4, 20.7, 22.8, 26.2, 29.0, 30.5, and 36.9. Stereochemistry of all amino acids in the acid hydrolyzate was assigned as L.

Partial Reduction and Alkylation of APA

A 300 μg portion (80 nmol) of APA was treated with 2.5 μl of TBP in MeCN-H_2O-TFA (60:40:0.1, 250 μl) for 15 min at 60ºC. The product gave only one peak other than the unreacted APA in reversed-phase HPLC using a linear gradient of MeCN-H_2O-TFA (40:60:0.1 to 60:40:0.1). The peak of the reduction product was collected and immediately treated with a solution of 2.2M iodoacetamide (200 μl, 0.5 M tris-acetate containing EDTA disodium salt [pH 8.0]) at 65ºC for 1 min. The reaction mixture was purified by reversed-phase HPLC as mentioned above. The molecular weight of the purified product [*m/z* 3958.6 $(M+Na)^+$] indicated introductions of two carboxyamidomethyl groups. The partially alkylated peptide was further treated with a mixture of TBP and 4-VP and the reaction mixture was purified by reversed-phase HPLC to afford a derivative, which had two carboxamidomethyl and four pyridylethyl groups as confirmed by the MALDI-TOFMS analysis [*m/z* 4360.6 $(M+H)^+$]. This peptide was subjected to protein sequence analysis to reveal the presence of carboxymethylated cysteine at residues 2 and 18.

Structure Calculations

Three hundred distance constraints were obtained from the 120 ms and 300 ms mixing time NOESY spectra recorded in CD_3OH. The cross peaks were categorized into four classes according to their intensities corresponding to upper bound interproton distance restraints of 2.5, 3.0, 4.0, and 5.0 Å. Pseudo-atoms were applied for methyl, methylene, and aromatic protons according to a standard method [22]. Nineteen dihedral angle constraints were generated from the $^3J_{NH\text{-}H\alpha}$ values which were determined by the DQF-COSY spectrum: the ϕ angles were constrained in the range of −120º ± 30º when the $^3J_{NH\text{-}H\alpha}$ values were larger than 8.0 Hz. A final set of 200 structures was calculated using the standard torsion angle simulated annealing protocol incorporated within the program CNS [16]. The 20 lowest energy structures were used to represent the solution structure of APA. Deviations value from idealized geometry of bond lengths, bond angles, and impropers were 0.0018 ± 0.0002 (Å), 0.42 ± 0.01 (º), and 0.20 ± 0.02 (º), respectively. Average pairwise RMSD value of heavy atoms and backbone atoms were 0.78 and 0.27 (Å), respectively.

Enzyme Inhibition Assay

A 90 μl portion of 4.45 mM solution of 2′-(4-methylumbelliferyl)-α-D-N-acetylneuraminic acid in 0.1 M NaOAc buffer (pH 4.2) was added to a 90 μl portion of 2.25×10^{-3} unit of sialidase (from *Clostridium perfringens*, Sigma N-2876) in 0.1 M NaOAc buffer (pH 4.2) and a test solution in DMSO (20 μl). The mixture was incubated at 37ºC for 30 min [23], and the amount of 4-methylumbelliferone (4%MU) released was measured by fluorescence at 450 nm following an excitation at 360 nm. The kinetic analysis of the inhibition of sialidase from *Clostridium perfringens* was carried out using the enzyme and buffer described above. The release of 4-MU was measured at 5 min intervals for 60 min using three substrate concentrations (0.013, 0.2, and 0.04 mM) and five inhibitor concentrations (13, 26, 39, 52, and 65 nM). The Lineweaver-Burk and Dixon analyses were conducted by the program "Michaelis-Menten protocol" using a Molecular Device Spectra MAX GEMINI apparatus.

Supplemental Data

Supplemental Data including Eight Figures may be found at http://www.chembiol.com/cgi/content/full/13/6/569/DC1/.

Acknowledgments

We are grateful to Dr. Kirk R. Gustafson and Dr. Thomas J. Turbyville, National Cancer Institute at Frederick, for reading the manuscript. We thank Professor Yasuo Suzuki, The University of Shizuoka, for a generous gift of the influenza virus. This work was partly supported by grant-in-aids from the Japan Society of Promotion of Science.

Received: January 18, 2006
Revised: April 5, 2006
Accepted: May 9, 2006
Published: June 23, 2006

References

1. Achyutha, K.E., and Achyuthanb, A.M. (2001). Comparative enzymology, biochemistry and pathophysiology of human exo-α-sialidases (neuraminidases). Comp. Biochem. Physiol. *B129*, 29–64.
2. Galen, J.E., Ketley, J.M., Fasano, A., Richardson, S.H., Wasserman, S.S., and Kaper, J.B. (1992). Role of Vibrio-cholerae neuraminidase in the function of cholera-toxin. Infect. Immun. *60*, 406–415.
3. von Itzstein, M., Wu, W.Y., Kok, G.B., Pegg, M.S., Dyason, J.C., Jin, B., Van Phan, T., Synthe, M.L., White, H.F., Oliver, S.W., et al. (1993). Rational design of potent sialidase-based inhibitors of influenza virus replication. Nature *363*, 418–423.
4. Umezawa, H., Aoyagi, T., Komiyama, T., Morishima, H., and Hamada, M. (1974). Purification and characterization of a sialidase inhibitor, siastatin, produced by Streptomyces. J. Antibiot. *27*, 963–969.
5. Nohara-Uchida, K., and Kaya, K. (1988). Inhibitory effect of taurolipids on Clostridium perfringens sialidase. J. Biochem. (Tokyo) *103*, 840–842.
6. Nakao, Y., Takada, K., Matsunaga, S., and Fusetani, N. (2001). Calyceramides A–C: neuraminidase inhibitory sulfated ceramides from the marine sponge Discodermia calyx. Teterahedron *57*, 3013–3017.
7. Takada, K., Nakao, Y., Matsunaga, S., and Fusetani, N. (2002). Nobiloside, a new neuraminidase inhibitory triterpenoidal saponin from the marine sponge *Erylus nobilis*. J. Nat. Prod. *65*, 411–413.
8. Bundi, A., and Wüthrich, K. (1979). ^{1}H NMR parameters of the common amino-acid residues meaured in aqueous-soutions of the linear tetrapeptides H-Gly-Gly-X-L-Ala-OH. Biopolymers *18*, 285–297.
9. Schwarzinger, S., Kroon, G.J.A., Foss, T.R., Chung, J., Wright, P.E., and Dyson, H.J. (2001). Sequence-Dependent Correction of Random Coil NMR Chemical Shifts J. J. Am. Chem. Soc. *123*, 2970–2978.
10. Wuthrich, K. (1986). NMR of Proteins and Nucleic Acids (New York: John Wiley & Sons).
11. Chazin, W.J., and Wright, P.E. (1987). A modified strategy for identification of 1H spin systems in proteins. Biopolymers *26*, 973–977.
12. Wishart, D.S., Sykes, B.D., and Richards, F.M. (1992). The chemical shift index: a fast and simple method for the assignment of protein secondary structure through NMR spectroscopy. Biochemistry *31*, 1647–1651.
13. Wishart, D.S., and Sykes, B.D. (1994). The ^{13}C chemical-shift index: a simple method for the identification of protein secondary structure using ^{13}C chemical-shift data. J. Biomol. NMR *4*, 171–180.
14. Klaus, W., Broger, C., Gerber, P., and Senn, H. (1993). Determination of the disulphide bonding pattern in proteins by local and global analysis of nuclear magnetic resonance data. J. Mol. Biol. *232*, 897–906.
15. Gray, W.R. (1993). Disulfide structures of highly bridged peptides: a new strategy for analysis. Protein Sci. *2*, 1732–1748.

16. Brunger, A.T., Clore, G.M., Delano, W.L., Gros, P., Grosse-kunstleve, R.W., Jiang, J.-S., Kuszewski, J., Nilges, N., Pannu, N.S., Read, R.J., et al. (1998). Crystallography & NMR System: A New Software for Macromolecular Structure Determination. Acta Crystallogr. D Biol. Crystallogr. *54*, 905–921.
17. Craik, D.J., Daly, N.L., and Waine, C. (2001). The cystine knot motif in toxins and implications for drug design. Toxicon *39*, 43–60.
18. Olivera, B.M., and Cruz, L.J. (2001). Conotoxins, in retrospect. Toxicon *39*, 7–14.
19. O'Keefe, B.R. (2000). Biologically active proteins from natural product extracts. J. Nat. Prod. *64*, 1373–1381.
20. Le, Q.M., Kiso, M., Someya, K., Sakai, Y.T., Nguyen, T.H., Nguyen, K.H.L., Pham, N.D., Ngyen, H.H., Yamada, S., Muramoto, Y., et al. (2005). Isolation of drug-resistant H5N1 virus. Nature *437*, 1108.
21. Piotto, M., Saudek, V., and Sklenar, V. (1992). Gradient-tailored excitation for single-quantum NMR spectroscopy of aqueous solutions. J. Biomol. NMR *2*, 661–665.
22. Wuthrich, K., Billeter, M., and Braun, W. (1983). Pseudostructures for the 20 common amino acids for use in studies of protein conformations by measurements of intramolecular proton-proton distance constraints with nuclear magnetic resonance. J. Mol. Biol. *169*, 949–961.
23. Potier, M., Mameli, L., Bélisle, M., Dallaire, L., and Melançon, S.B. (1979). Fluorometric assay of neuraminidase with a sodium (4-methylumbelliferyl-α-D-*N*-acetylneuraminate) substrate. Anal. Biochem. *94*, 287–296.
24. Shon, K.J., Hasson, A., Spira, M.E., Cruz, L.J., Gray, W.R., and Olivera, B.M. (1994). δ-Conotoxin GmVIA, a Novel Peptide from the Venom of Conus gloriamaris. Biochemistry *33*, 11420–11425.
25. Hillyard, D., Olivera, B.M., Woodward, S., Corpuz, G., Gray, W., Ramilo, C., and Cruz, L. (1989). A molluskivorous Conus toxin: conserved frameworks in conotoxins. Biochemistry *28*, 358–361.
26. Olivera, B.M., McIntosh, J.M., Cruz, L.J., Luque, F.A., and Gray, W.R. (1984). Purification and sequence of a presynaptic peptide toxin from Conus geographus venom. Biochemistry *23*, 5087–5090.
27. Olivera, B.M., Cruz, L.J., de Santos, V., LeCheminant, G.W., Griffin, D., Zeikus, R., McIntosh, J.M., Galyean, R., Varga, J., Gray, W.R., et al. (1987). Neuronal calcium channel antagonists. Discrimination between calcium channel subtypes using ω-conotoxin from Conus magus venom. Biochemistry *26*, 2086–2090.
28. Ramilo, C.A., Zafaralla, G.C., Nadasdi, L., Hammerland, L.G., Yoshikami, D., Gray, W.R., Kristipati, R., Ramachandran, J., Miljanich, G., Olivera, B.M., et al. (1992). Novel α- and ω-conotoxins and Conus striatus venom. Biochemistry *31*, 9919–9926.
29. Liang, S.P., Zhang, D.Y., Pan, X., Chen, Q., and Zhou, P.A. (1993). Properties and amino acid sequence of huwentoxin-I, a neurotoxin purified from the venom of the Chinese bird spider Selenocosmia huwena. Toxicon *31*, 969–978.
30. Peng, K., Shu, Q., Liu, Z., and Liang, S. (2002). Function and solution structure of huwentoxin-IV, a potent neuronal tetrodotoxin (TTX)-sensitive sodium channel antagonist from Chinese bird spider *Selenocosmia huwena*. J. Biol. Chem. *277*, 47564–47571.
31. Koradi, R., Billeter, M., and Wuthrich, K. (1996). MOLMOL: a program for display and analysis of macromolecular structures. J. Mol. Graph. *14*, 51–55.